

# Stimulated emission and ultrafast carrier relaxation in InGaN multiple quantum wells

Ümit Özgür, and Henry O. Everitt<sup>a)</sup>

*Department of Physics, Duke University, Durham, NC 27708*

Stacia Keller and Steven P. DenBaars

*Department of Electrical Engineering and Materials Science, University of California, Santa Barbara, CA*

(October 31, 2018)

Stimulated emission (SE) was measured from two InGaN multiple quantum well (MQW) laser structures with different In compositions. SE threshold power densities ( $I_{th}$ ) increased with increasing QW depth ( $x$ ). Time-resolved differential transmission measurements mapped the carrier relaxation mechanisms and explained the dependence of  $I_{th}$  on  $x$ . Carriers are captured from the barriers to the QWs in  $< 1$  ps, while carrier recombination rates increased with increasing  $x$ . For excitation above  $I_{th}$  an additional, fast relaxation mechanism appears due to the loss of carriers in the barriers through a cascaded refilling of the QW state undergoing SE. The increased material inhomogeneity with increasing  $x$  provides additional relaxation channels outside the cascaded refilling process, removing carriers from the SE process and increasing  $I_{th}$ .

78.47.+p,78.66.Fd,78.45.+h,78.67.De

Recent advances in the growth of group-III nitride heterostructures have made it possible to manufacture efficient green, blue, and ultraviolet emitters and detectors.<sup>1–3</sup> Carrier dynamics in such device structures are beginning to be understood through the use of high power, short pulse, regenerative and optical parametric amplifiers.<sup>4–7</sup> In this paper, stimulated emission (SE) in InGaN multiple quantum well (MQW) laser structures with differing QW depths is explored. SE threshold power densities increase with increasing QW depth, and ultrafast measurements of carrier dynamics reveal why.

Two different InGaN MQW samples, differing primarily by QW In composition ( $x$ ), were grown on c-plane sapphire in a modified two flow metalorganic chemical vapor deposition (MOCVD) reactor.<sup>8</sup> Both samples have  $\sim 2$   $\mu\text{m}$  thick GaN:Si base layers. The 12% sample consists of 10 periods of 8.2 nm/3.4 nm  $\text{In}_{0.07}\text{Ga}_{0.93}\text{N}:\text{Si}/\text{In}_{0.12}\text{Ga}_{0.88}\text{N}$  QWs and is capped with a 100 nm thick GaN:Si layer. The 23% sample consists of 12 periods of 10 nm/3.5 nm  $\text{In}_{0.03}\text{Ga}_{0.97}\text{N}:\text{Si}/\text{In}_{0.23}\text{Ga}_{0.77}\text{N}$  QWs and is capped with 16 nm thick  $\text{Al}_{0.10}\text{Ga}_{0.90}\text{N}$  and 40 nm thick GaN:Si layers. The In compositions and the QW/barrier thicknesses are determined by high resolution X-Ray measurements. Material inhomogeneities, which arise from QW thickness fluctuations, compositional fluctuations, and In phase separation, have previously been observed to increase with increasing  $x$  and will be shown to play an important role in carrier relaxation and emission processes.<sup>9,10</sup>

Fig. 1 shows the cw-PL for 3.81 eV low intensity (300W Xe lamp) and moderate intensity (25mW HeCd laser at 325 nm) excitations, and time-integrated PL (TI-PL) with a high intensity ( $\sim 15$   $\mu\text{J}/\text{cm}^2$ ) pulsed 3.31 eV excitation for both MQW samples. PL for the 12% sample shows a single peak at 3.01 eV for both Xe lamp (not shown) and HeCd excitations. The 23% sample shows at

least two well-defined PL peaks for Xe-Lamp and HeCd laser excitation, the higher energy of which (2.52 eV) is assigned as the main PL from the QWs. The lower energy PL peak is associated with impurity (yellow) emission. For both samples, TI-PL from spontaneous emission (SPE) blueshifted for with increasing pump pulse intensity (Fig. 1) due to band filling and piezoelectric (PZE) field screening by the increasing number of laser-induced carriers.<sup>9</sup> The intensity-dependent blueshifts and PL linewidths increased with increasing  $x$ , indicating a greater role of inhomogeneities.

Cw-absorption measurements (Fig. 1) revealed the 3D barrier energies as 3.23 eV and 3.29 eV for the 12% and 23% samples, respectively. Although the 12% sample showed no remarkable QW band edge absorption, a PLE edge at the confined QW energy is weakly visible at room temperature (3.11 eV) and clearly visible at 77 K (3.14 eV). By contrast, the QW band edge is clearly observed for the 23% sample at 2.93 eV for both cw-absorption and PLE measurements. More importantly, the PLE signal was much broader for the 23% sample and extended to localized states at least 200 meV below the QW band edge. The broadening of the PLE, the Stokes-like shift between the QW band edge and the emission energy, and the number of localized states below the QW band edge clearly increased with increasing  $x$ , another consequence of increased material inhomogeneities and carrier localization.

For normal incidence pulsed excitation at moderate pump densities ( $> 100$   $\mu\text{J}/\text{cm}^2$ ), stimulated emission (SE) is observed from the edge parallel to the sample surface. The SE peaks for both samples appear near the QW band edge, indicating that the SE originates from the lowest energy QW confined states. Spectrally-integrated emission and linewidths were measured as a function of the average pump density to obtain  $I_{th}$ .<sup>11</sup> For the 12% sample, a broad SE peak appeared slightly blueshifted (20

meV) from the PL peak. In contrast, the SE peak for the 23% sample (2.90 eV) appeared 200 meV bluer than the PL peak. The linewidth of the SE peak for the 23% sample ( $>70$  meV) is remarkably larger than the linewidth for the 12% sample ( $\sim 30$  meV), again a consequence of material inhomogeneities.

SE thresholds ( $I_{th}$ ) increased with  $x$  (90, and 160  $\mu\text{J}/\text{cm}^2$  for the 12% and 23% samples, respectively), contradicting earlier observations that  $I_{th}$  decreased with increasing QW depth.<sup>6,12</sup> In order to further investigate this behavior, non-degenerate time-resolved differential transmission (TRDT) spectroscopy was applied to measure carrier dynamics at room temperature. A Ti:Sapphire laser-seeded Quantronix Titan regenerative amplifier (RGA) with  $\sim 1.8$  mJ,  $\sim 100$  fs pulses at 800 nm was used. Half of the RGA output power is used to pump a Quantronix TOPAS optical parametric amplifier (OPA). The signal output from the tunable OPA is frequency quadrupled and used as the pump in the TRDT experiment. The other half of the RGA output is frequency doubled in a BBO crystal and focused on a quartz cell filled with  $\text{D}_2\text{O}$  to generate a broadband continuum probe. The pump beam is delayed with respect to the probe beam using a retroreflector mounted on a 1  $\mu\text{m}$ -resolution translational stage. The probe, transmitted through the sample, is then collected by a spectrometer with a liquid nitrogen cooled charge-coupled device camera.

To examine the relaxation of the total population of carriers, TRDT signals are spectrally integrated (SI) over all energies where photoexcited carriers were observed (Fig. 2). For excitation energies near the barrier band edge and power densities above  $I_{th}$ , both samples show an initial fast decay followed by a much slower relaxation. SI-TRDT data were fit by a bi-exponential decay function,  $F e^{-t/\tau_F} + S e^{-t/\tau_S}$ , where  $\tau_F$  and  $\tau_S$  are the decay constants, and  $F$  and  $S$  are the magnitudes, for the fast and slow decaying components, respectively. As the excitation density decreased,  $F$  decreased and  $\tau_F$  slowed, while  $S$  and  $\tau_S$  were unchanged (Fig. 2). The fast decaying component in the SI-TRDT data is caused by the accelerated relaxation of carriers through SE.<sup>5,7</sup> After  $\sim 10$  ps the SE ends, leaving only the much slower decaying component due to carrier recombination and spontaneous emission.

Spectrally-resolved TRDT (SR-TRDT) data for the 12% and 23% samples further elucidates the carrier redistribution and relaxation processes, as shown in Fig. 3.<sup>13</sup> For excitation densities below  $I_{th}$  in the 12% sample ( $I_{th}(12\%)$ ), photoexcited carriers relax to the barrier band edge in  $<1$  ps, resulting in a broad distribution (160 meV) of carriers in the QWs centered at energies that increasingly redshift below the barriers with increasing time (Fig. 3a). The arrival of carriers at the QW band edge (3.11 eV)  $\sim 300$  fs after carrier accumulation at the barriers (3.22 eV) indicates the rate of carrier capture from the 3D barrier states into the 2D QW states.<sup>4,5</sup> For excitation densities above  $I_{th}(12\%)$ , the larger number

of photoexcited carriers relax in a similar manner, except that the broad carrier distribution is centered at, not below, the barrier energy (Fig. 3b). This suggests that the QW states are saturated at high excitation densities and that excess photoexcited carriers accumulate in the 3D barrier states. For both excitations, the blue edge of the carrier distribution begins to decay after 1 ps, but the red edge remains almost constant until 400 ps. The rate of blue edge decay is significantly faster for the above  $I_{th}$  excitation than below (Fig. 3b), explaining the pump intensity-dependent behavior of the fast component in the SI-TRDT (Fig. 2a). It is apparent that during the SE process, carriers cascade to refill the emission-emptied QW states from higher energy 3D barrier states and 2D QW states.<sup>5,7</sup> After SE ends, a much slower, pump intensity-independent decay and redshift is observed as the carriers are lost through recombination. By 400 ps, the carrier distribution is centered at the QW band edge (3.11 eV). The decay constant for the TRDT signal at the QW energy (3.11 eV) is  $0.66 \pm 0.06$  ps, which agrees with the slow SI-TRDT rate and the previously measured recombination time.<sup>4</sup>

SR-TRDT data for the 23% sample for excitation densities below (Fig. 3c) and above (Fig. 3d)  $I_{th}(23\%)$  presents a slightly different behavior. Since the localized and confined QW states are deeper, initial carrier accumulation is not observed at the barrier energy, and below  $I_{th}$  excitation produces a broader (420 meV) carrier distribution whose peak occurs near the QW band edge ( $\sim 2.93$  eV) in only 0.5 ps. The carriers arrive in the QWs (2.93 eV) 0.85 ps later than at the barriers (3.29 eV), indicating the carrier capture process is significantly slower than in the 12% sample. By contrast, for the above  $I_{th}(23\%)$  excitation, a wider and flatter carrier distribution is observed in 1 ps, extending from the barriers to the localized states below the QWs. As in the 12% sample, the blue edge of the carrier distribution is responsible for the fast component in Fig. 2b, which peaks in  $<1$  ps and quickly decays while SE is underway ( $<10$  ps). Likewise, the carrier distribution peak remains near the QW band edge, and carriers cascade from higher energy states to refill the SE-emptied QW states. After SE ends, the distribution continues to redshift slowly as carriers are lost through various decay channels. The carriers at the QW band edge are observed to decay much faster ( $0.32 \pm 0.05$  ns at 2.90 eV) than in the 12% sample. This occurs because, in addition to radiative decay, QW carriers in the 23% sample decay non-radiatively into the localized states as much as 200 meV below the QW band edge. Carrier decay is slower in these localized states ( $0.48 \pm 0.08$  ns at 2.84 eV) than at the QW band edge, suggesting that the presence of these localized states undermines the QW radiative emission process. As further evidence of the role of inhomogeneities in the 23% sample, note the long-lived induced absorption at the barrier energies, also due to carriers localized in traps after 10 ps.

For the 23% sample, then, localization in material in-

homogeneities plays a greater role in the carrier redistribution and relaxation processes. A larger percentage of carriers are trapped by the inhomogeneities at the barriers and in the localized states below the SE ( $\sim$ QW) energy, making them energetically unavailable to participate in the refilling process required to sustain SE. The increased importance of non-radiative relaxation produces carrier decay times at the QW band edge that are remarkably faster for the 23% than for the 12% sample. The combination of these effects leads to a greater variety of carrier relaxation channels and a commensurate increase of  $I_{th}$  (23%) over  $I_{th}$  (12%). These observations reconcile the apparently conflicting findings of Kwon *et al.* and Yablonskii *et al.* regarding the dependence of  $I_{th}$  on the QW depth.<sup>12,14</sup> In the former case, which concerns GaN/In<sub>x</sub>Ga<sub>1-x</sub>N MQWs with  $x < 13.3\%$ ,  $I_{th}$  is low, as reported here, because of the (reduced) material inhomogeneities. However,  $I_{th}$  was found to increase with decreasing  $x$  because of the increasing role of other non-radiative pathways.<sup>12</sup> In the latter case, emission from MQWs with unknown but larger  $x$  exhibits the same sort of increase in  $I_{th}$  with  $x$  as reported here. They similarly conclude that non-radiative processes involving (increased) inhomogeneities is responsible.<sup>14</sup> The transition for  $I_{th}$  behavior appears to occur at a critical value for  $x$  ( $\sim 0.20$ ), above which inhomogeneities, Stokes-like shifts, and radiative decay times are known to increase rapidly.<sup>9</sup>

This work was partially supported by ARO grant DAAG55-98-D-0002-0007.

Deguchi, D. Cohen, P. Kozodoy, S. B. Fleischer, S. Keller, J. S. Peck, J. E. Bowers, E. Hu, U. K. Mishra, L. A. Coldren, S. P. DenBaars, K. Wada, T. Sota, and S. Nakamura, *Mater. Sci. and Eng. B* **59**, 298 (1999).

- <sup>11</sup> Weak SE is still seen below  $I_{th}$  due to inhomogeneities and the nonuniform intensity profile of the pump spot.
- <sup>12</sup> Y. -H. Kwon, G. H. Gainer, S. Bidnyk, Y. H. Cho, J. J. Song, M. Hansen, and S. P. DenBaars, *Appl. Phys. Lett.* **75**, 2545 (1999).
- <sup>13</sup> Increased transmission at the GaN energy (3.41 eV) appears in both samples due to the AC Stark effect and two-photon absorption-induced carriers in the cap and buffer GaN layers.<sup>5</sup>
- <sup>14</sup> G. P. Yablonskii, E. V. Lutsenko, V. N. Pavlovskii, I. P. Marko, B. Schineller, M. Heuken, and K. Heime, *Mater. Sci. and Eng. B* **80**, 322 (2001).

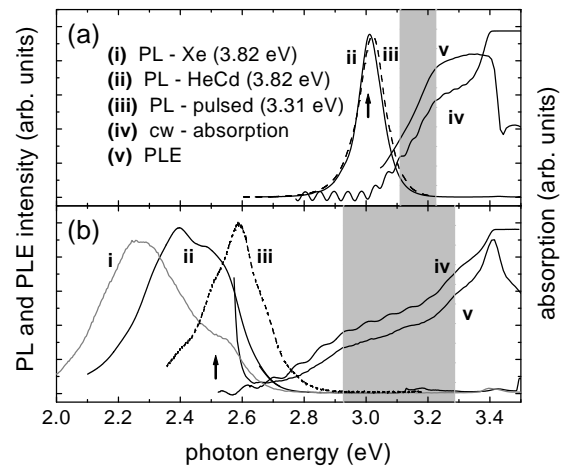


FIG. 1. Room temperature cw-PL using a Xe lamp source at 325 nm (i) and a HeCd laser (ii); time-integrated, below  $I_{th}$ , pulsed-PL (iii), Cw-absorption (iv), and PLE (v) for the (a) 12%, and (b) 23% MQW samples. The shaded regions show the states between the barrier and QW band edges. Arrows show the detection energies for the PLE.

- <sup>1</sup> S. Nakamura and G. Fasol, *The Blue Laser Diode*, Springer, Berlin 1997, and references therein.
- <sup>2</sup> S. Nakamura, M. Senoh, S. Nagahama, N. Iwasa, T. Yamada, T. Matsushita, H. Kiyoku, Y. Sugimoto, T. Kozaki, H. Umemoto, M. Sano, and K. Chocko, *Jpn. J. Appl. Phys., Part 2* **36**, L1568 (1997).
- <sup>3</sup> S. Nakamura, M. Senoh, N. Iwasa, and S. Nagahama, *Jpn. J. Appl. Phys.* **34**, L797 (1995).
- <sup>4</sup> Ü. Özgür, M. J. Bergmann, H. C. Casey, Jr., H. O. Everitt, A. C. Abare, S. Keller, and S. P. DenBaars, *Appl. Phys. Lett.* **77**, 109 (2000).
- <sup>5</sup> Ü. Özgür and H. O. Everitt, <http://xxx.lanl.gov/abs/cond-mat/0210214>, submitted to *Phys. Rev. B*.
- <sup>6</sup> Y. Kawakami, Y. Narukawa, K. Omae, S. Fujita, and S. Nakamura, *Appl. Phys. Lett.* **77**, 2151 (2000).
- <sup>7</sup> A. Satake, Y. Masumoto, T. Miyajima, T. Asatsuma, and M. Ikeda, *Phys. Rev. B* **60**, 16660 (1999).
- <sup>8</sup> S. Keller, S. F. Chichibu, M. S. Minsky, E. Hu, U. K. Mishra, and S. P. DenBaars, *J. Cryst. Growth* **195**, 258 (1998).
- <sup>9</sup> S. Chichibu, T. Sota, K. Wada, and S. Nakamura, *J. Vac. Sci. Technol. B* **16**, 2204 (1998).
- <sup>10</sup> S. F. Chichibu, A. C. Abare, M. P. Mack, M. S. Minsky, T.

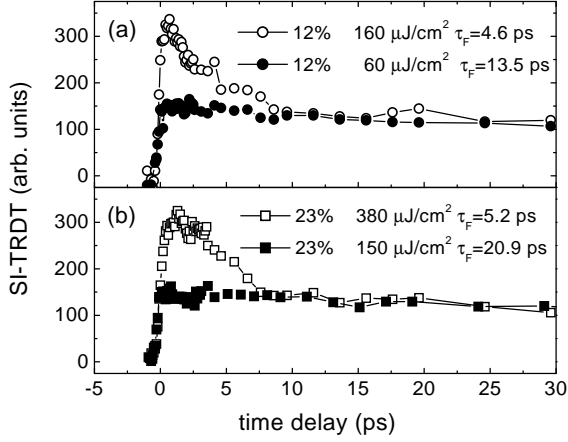


FIG. 2. SI-TRDT for the (a) 12% and (b) 23% MQW samples, excited at energies near the barrier band edge for densities above (open) and below (filled)  $I_{th}$ . Spectral integration occurred from the GaN band edge (3.40 eV) to below the In-GaN QWs (2.92 and 2.55 eV for the 12% and 23% samples, respectively).

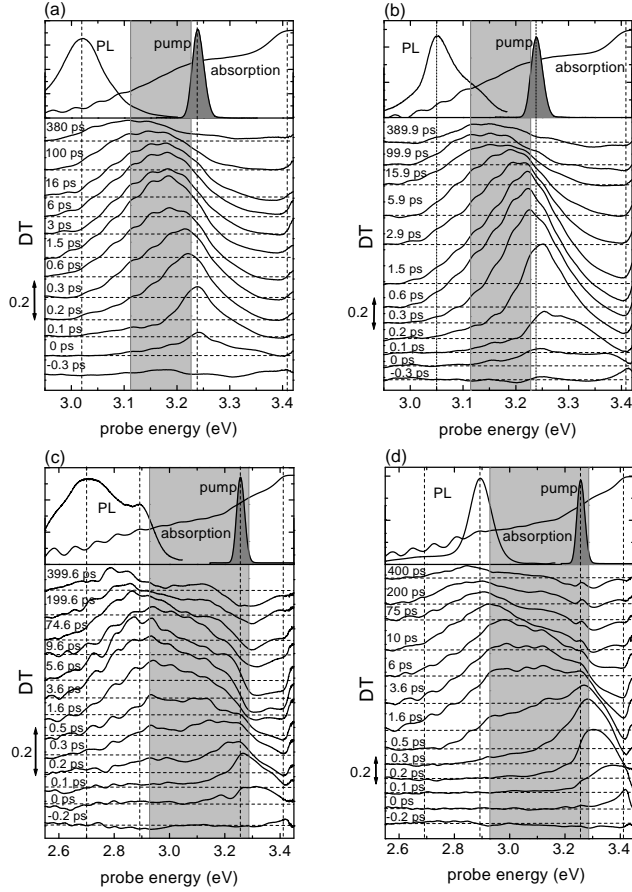


FIG. 3. SR-TRDT for (a) below ( $60 \mu\text{J}/\text{cm}^2$ ) and (b) above ( $160 \mu\text{J}/\text{cm}^2$ )  $I_{th}$  (12%), and (c) below ( $150 \mu\text{J}/\text{cm}^2$ ) and (d) above ( $380 \mu\text{J}/\text{cm}^2$ )  $I_{th}$  (23%). Shaded regions show the states between the barrier and the QW band edges.